



## King's Research Portal

DOI:

[10.1016/j.ejrad.2019.06.005](https://doi.org/10.1016/j.ejrad.2019.06.005)

*Document Version*

Peer reviewed version

[Link to publication record in King's Research Portal](#)

*Citation for published version (APA):*

Murphy, D. J., Royle, L., Chalampalakis, Z., Alves, L., Martins, N., Bassett, P., Breen, R., Nair, A., Bille, A., Chicklore, S., Cook, G. J., & Subesinghe, M. (2019). The effect of a novel Bayesian penalised likelihood PET reconstruction algorithm on the assessment of malignancy risk in solitary pulmonary nodules according to the British Thoracic Society guidelines. *European journal of radiology*, 117, 149-155.  
<https://doi.org/10.1016/j.ejrad.2019.06.005>

### **Citing this paper**

Please note that where the full-text provided on King's Research Portal is the Author Accepted Manuscript or Post-Print version this may differ from the final Published version. If citing, it is advised that you check and use the publisher's definitive version for pagination, volume/issue, and date of publication details. And where the final published version is provided on the Research Portal, if citing you are again advised to check the publisher's website for any subsequent corrections.

### **General rights**

Copyright and moral rights for the publications made accessible in the Research Portal are retained by the authors and/or other copyright owners and it is a condition of accessing publications that users recognize and abide by the legal requirements associated with these rights.

- Users may download and print one copy of any publication from the Research Portal for the purpose of private study or research.
- You may not further distribute the material or use it for any profit-making activity or commercial gain
- You may freely distribute the URL identifying the publication in the Research Portal

### **Take down policy**

If you believe that this document breaches copyright please contact [librarypure@kcl.ac.uk](mailto:librarypure@kcl.ac.uk) providing details, and we will remove access to the work immediately and investigate your claim.

Manuscript Number: EJRD-19-00091R2

Title: The effect of a novel Bayesian Penalised Likelihood PET reconstruction algorithm on the assessment of malignancy risk in pulmonary nodules according to the British Thoracic Society guidelines

Article Type: Research Article

Section/Category: Nuclear Medicine and Oncology

Keywords: Solitary pulmonary nodule;  
Fluorodeoxyglucose F18;  
Positron emission tomography computed tomography;  
Image reconstruction;  
Risk assessment;

Corresponding Author: Dr. David J Murphy, MB BCh BAO, MRCPI, FFRCSI, FRCR

Corresponding Author's Institution: St Vincent's University Hospital

First Author: David J Murphy, MB BCh BAO, MRCPI, FFRCSI, FRCR

Order of Authors: David J Murphy, MB BCh BAO, MRCPI, FFRCSI, FRCR;  
Leanne Royle; Zach Chalampalakakis; Luis Alves; Nuno Martins; Paul Bassett;  
Ronan Breen; Arjun Nair; Andrea Bille; Sugama Chicklore; Gary J Cook;  
Manil Subesinghe

#### Abstract: Purpose

British Thoracic Society (BTS) guidelines advocate using FDG PET-CT with the Herder model to estimate malignancy risk in solitary pulmonary nodules (SPNs). Qualitative and semi-quantitative assessment of SPN uptake is based upon analysis of Ordered Subset Expected Maximisation (OSEM) PET images. Our aim was to assess the effect of Bayesian Penalised Likelihood (BPL) PET reconstruction on the assessment of SPN FDG uptake and estimation of malignancy risk (Herder score).

#### Methods

Subjects with SPNs who underwent FDG PET-CT between 2014-2017, with histological confirmation of malignancy or histological/imaging follow-up confirmation of benignity were included. Two blinded readers independently classified SPN uptake on both OSEM and BPL (BTS score; 1 = none; 2 =  $\leq$  mediastinal blood pool (MBP); 3 =  $>$ MBP but  $\leq$  2x liver; 4 =  $>$ 2x liver), with resultant calculation of the Herder score (%) for both reconstructions.

#### Results

97 subjects with 75 (77%) malignant SPNs were included. BPL increased the BTS score in 25 (26%) SPNs; 9 SPNs (7 malignant) increased from BTS score 2 to 3, 16 (13 malignant) from BTS score 3 to 4, with a mean Herder score increase of  $18\pm 22\%$ . The mean Herder score for all SPNs with BPL was higher than OSEM ( $73\pm 29$  vs  $68\pm 32\%$ ,  $p=0.001$ ). There was no difference

in Herder model diagnostic performance between BPL and OSEM, with similar areas under the curve (0.84 vs 0.83,  $p=0.39$ ).

#### Conclusion

BPL increases the Herder score in 26% of SPNs compared to OSEM but does not alter the diagnostic performance of the Herder model.

Dear Dr Byrne,

We thank you for taking the time to consider our submission, and for your reviewers' considered comments. We have endeavoured to address these comments in our revised submission.

Please find details of our response to the reviewers' comments presented below. The reviewer comments are presented in bold, with the authors' response following in italics.

We hope you consider our revised submission suitable for publication.

**Reviewers' comments:**

**Reviewer #1: Thank you for the deep review, however I have one more comment. I thinkt the Table 3 in its current form is poorly arranged and recommend to summarize the informantion and include in another table or leave only as a text.**

*Thank you for this comment. Based on this, we have removed this table from our revised submission-the information in the table is already summarized in the results section of the manuscript*

**Reviewer #2: after explanation of the comments and questions, I can recommend the manustcript for publication**

*We thank the reviewer for their comment.*

**Conflicts of Interest:** No author declares a conflict of interest.

**Ethical approval:** Ethical approval was obtained for this retrospective study by the local institutional review board. There were no additional procedures performed in human or animal participants.

**Informed consent:** Informed consent was waived by the IRB for this retrospective study.

# *European Journal of Radiology*

## Author Form

All manuscripts submitted to the *European Journal of Radiology* must be accompanied by this form. Please scan the form and transmit it to the Editorial Office via EES with the manuscript. If you are unable to do this, please contact the Editorial Office at [ejr@elsevier.com](mailto:ejr@elsevier.com) to organise an alternative way of sending the form to the Journal.

**Title of Manuscript:**

The effect of a novel Bayesian Penalised Likelihood PET reconstruction algorithm on the assessment of malignancy risk in pulmonary nodules according to the British Thoracic Society guidelines

Contribution	Author(s)
Study concepts:	DJM, CJC, MS
Study design:	DJM, CJC, MS
Data acquisition:	DJM, LR, ZC, LA, NM, RB, AN, AB, SC, MS
Quality control of data and algorithms:	DJM, MS
Data analysis and interpretation:	DJM, PB, MS
Statistical analysis:	DJM, PB, GJC, MS
Manuscript preparation:	DJM, PB, MS
Manuscript editing:	DJM, PB, AN, GJC, MS
Manuscript review:	LR, ZC, LA, NM, PB, RB, AN, AB, AC, GJC

**Ethical Approval for Research:** YEs.

**External Funding:** Yes

**Source of Funding:** King's College London / University College London Comprehensive Cancer Imaging Centres funded by Cancer Research UK and Engineering and Physical Sciences Research Council in association with the Medical Research Council and the Department of Health (C1519/A16463) and the Wellcome Trust EPSRC Centre for Medical Engineering at King's College London (WT203148/Z/16/Z).

**Name of Principal Investigator:** MS

(If funded, please include a statement as to the role of the study sponsor at end of manuscript under a heading 'Role of the Funding Source')

**Possible Conflict of Interest:** No

(Please ensure that a 'Conflict of Interest' statement is included in your manuscript)

**Number of Tables:** 3

**Number of Figures:** 5

**Name and Title of Corresponding Author:** David J Murphy, Consultant Cardiothoracic Radiologist

**Address:** St Vincent's University Hospital

**Address:** Elm Park


**Postcode and country:** Dublin 4, Ireland

**Tel No:** 00353-1-2214000

**Fax No:** 00353-1-2214252

**Email:** murphy.84@gmail.com

**"I confirm that all the authors have made a significant contribution to this manuscript, have seen and approved the final manuscript, and have agreed to its submission to the *European Journal of Radiology*".**

**Signed** (corresponding author): 

**Date:** 12/1/2019

## Highlights

- Herder score for lung nodule FDG uptake on PET/CT has good inter-reader agreement
- Novel BPL PET reconstruction increases the Herder score in 26% of nodules
- Herder model diagnostic performance of BPL and standard OSEM PET show no difference

**The effect of a novel Bayesian Penalised Likelihood PET reconstruction algorithm on the assessment of malignancy risk in pulmonary nodules according to the British Thoracic Society guidelines**

DJ Murphy<sup>a,b</sup>, L Royle<sup>c</sup>, Z Chalampalakakis<sup>a</sup>, L Alves<sup>a</sup>, N Martin<sup>a</sup>, P Bassett<sup>d</sup>, R Breen<sup>e</sup>, A Nair<sup>c</sup>, A Bille<sup>f</sup>, S Chicklore<sup>a,b</sup>, G J Cook<sup>a,b</sup>, M Subesinghe<sup>a,b</sup>

<sup>a</sup>*King's College London & Guy's and St. Thomas' PET Centre, St. Thomas' Hospital, London, UK*

<sup>b</sup>*School of Biomedical Engineering and Imaging Sciences, King's College London, London, UK*

<sup>c</sup>*Department of Radiology, Guy's and St. Thomas' NHS Foundation Trust, London, UK*

<sup>d</sup>*Statsconsultancy Ltd., London, UK*

<sup>e</sup>*Department of Respiratory Medicine, Guy's and St. Thomas' NHS Foundation Trust, London, UK*

<sup>f</sup>*Department of Cardiothoracic Surgery, Guy's and St. Thomas' NHS Foundation Trust, London, UK*

**Corresponding author (present address):**

David J Murphy,  
St Vincent's University Hospital,  
Elm Park,  
Dublin 4, Ireland  
Tel: +353-1-2214000  
Email: david.murphy@st-vincent's.ie

**Conflicts:** We have no conflicts to disclose.

**Funding:** The authors acknowledge support from the King's College London / University College London Comprehensive Cancer Imaging Centres funded by Cancer Research UK and Engineering and Physical Sciences Research Council in association with the Medical Research Council and the Department of Health (C1519/A16463) and the Wellcome Trust EPSRC Centre for Medical Engineering at King's College London (WT203148/Z/16/Z).

**Word count:** 3,978 (main manuscript including abstract, excluding key words reference and figure/table legends)



The effect of a novel Bayesian Penalised Likelihood PET reconstruction algorithm on the assessment of malignancy risk in solitary pulmonary nodules according to the British Thoracic Society guidelines

**Abstract**

**Purpose**

British Thoracic Society (BTS) guidelines advocate using FDG PET-CT with the Herder model to estimate malignancy risk in solitary pulmonary nodules (SPNs). Qualitative and semi-quantitative assessment of SPN uptake is based upon analysis of Ordered Subset Expected Maximisation (OSEM) PET images. Our aim was to assess the effect of Bayesian Penalised Likelihood (BPL) PET reconstruction on the assessment of SPN FDG uptake and estimation of malignancy risk (Herder score).

**Methods**

Subjects with SPNs who underwent FDG PET-CT between 2014-2017, with histological confirmation of malignancy or histological/imaging follow-up confirmation of benignity were included. Two blinded readers independently classified SPN uptake on both OSEM and BPL (BTS score; 1 = none; 2 = ≤ mediastinal blood pool (MBP); 3 = >MBP but ≤ 2x liver; 4 = >2x liver), with resultant calculation of the Herder score (%) for both reconstructions.

**Results**

97 subjects with 75 (77%) malignant SPNs were included. BPL increased the BTS score in 25 (26%) SPNs; 9 SPNs (7 malignant) increased from BTS score 2 to 3, 16 (13 malignant) from BTS score 3 to 4, with a mean Herder score increase of 18±22%. The mean Herder score for all SPNs with BPL was higher than OSEM (73±29 vs 68±32%, p=0.001). There was no difference in Herder model diagnostic performance between BPL and OSEM, with similar areas under the curve (0.84 vs 0.83, p=0.39).

**Conclusion**

BPL increases the Herder score in 26% of SPNs compared to OSEM but does not alter the diagnostic performance of the Herder model.

## Keywords

Solitary pulmonary nodule;

Fluorodeoxyglucose F18;

Positron emission tomography computed tomography;

Image reconstruction;

Risk assessment;

## Abbreviations

### Area under the curve (AUC)

- 1
- 2 BPL= Bayesian Penalised Likelihood
- 3
- 4 BTS= British Thoracic Society
- 5
- 6
- 7 CT= Computed tomography
- 8
- 9
- 10 FDG= 2-deoxy-2-[<sup>18</sup>F]fluoro-D-glucose
- 11
- 12 ICC= Intra-class correlation
- 13
- 14
- 15 MBP=Mediastinal blood pool
- 16
- 17 OSEM=Ordered Subset Expected Maximisation
- 18
- 19
- 20 PET= Positron emission tomography
- 21
- 22
- 23 PSF= Point spread function
- 24
- 25 ROC= Receiver operating characteristic
- 26
- 27
- 28 SPN= Solitary pulmonary nodule
- 29
- 30 SUV= Standardised uptake value
- 31
- 32
- 33
- 34
- 35
- 36
- 37
- 38
- 39
- 40
- 41
- 42
- 43
- 44
- 45
- 46
- 47
- 48
- 49
- 50
- 51
- 52
- 53
- 54
- 55
- 56
- 57
- 58
- 59
- 60
- 61
- 62
- 63
- 64
- 65

## Introduction:

Recent guidance issued by the British Thoracic Society (BTS) in 2015 [1] on the investigation and management of solitary pulmonary nodules (SPNs) advocates the use of clinico-radiological risk prediction models to guide clinical decision making for patients who have a SPN identified and confirmed on computed tomography (CT) imaging.

Following an initial CT scan, an estimate of malignancy risk ( $< 10\%$  or  $> 10\%$ ) is made using the Brock model [2], which encompasses findings on the CT scan (nodule size, type, location, count, spiculation, emphysema) along with clinical parameters (age, gender, family history of lung cancer). Patients with a greater than 10% risk of malignancy following their CT scan are recommended to undergo a 2-deoxy-2- $^{18}\text{F}$ fluoro-D-glucose (FDG) positron emission tomography (PET)-CT scan for further risk stratification ( $<10\%$ , 10-70% or  $>70\%$  risk of malignancy), using the Herder model [3], which incorporates the degree of FDG uptake within a SPN, along with other clinico-radiological parameters (age, smoking status, history of extra-thoracic cancer, nodule size, location and spiculation). The incorporation of FDG uptake adds incremental benefit to diagnostic accuracy, increasing the area under the receiver operating characteristic (ROC) curve from 0.79 to 0.92 [3].

The Herder model, an accurate model incorporating PET for predicting malignancy in SPNs, has been validated in a UK population [4]. Its application is dependent on the accurate classification of FDG uptake in a SPN using qualitative assessment with an ordinal scale as follows; absent, faint, moderate, or intense. Herder et al. [3] did not provide detail regarding the definition of these levels of FDG uptake, although other studies have [5,6]. The BTS guideline development group adapted and derived a 4-point scale based on the above, to enable use with the Herder model (**Table 1, Figure 1**).

Importantly, the degree of FDG uptake within SPNs is based upon analysis of PET images reconstructed using a standard PET reconstruction algorithm, Ordered Subset Expected Maximisation (OSEM). OSEM is an iterative reconstruction algorithm, with each successive iteration producing an image estimate closer to the true image, i.e. convergence. However, with each iteration, image noise increases and eventually reaches unacceptable levels whereby noise dominates. For this reason, OSEM is terminated after a set

number of iterations resulting in an underconverged image with quantification underestimation and resultant underestimation of standardised uptake values (SUVs) [7,8].

In recent years, novel PET reconstruction algorithms have been introduced to improve image quality through increasing signal-to-noise ratio. GE Healthcare have introduced a (Bayesian Penalised Likelihood) BPL iterative PET reconstruction algorithm, Q.Clear, which is available on modern GE Healthcare PET-CT scanners [9]. This reconstruction permits an increased number of iterations without an accompanying increase in noise due to the use of a penalty function, which acts as a noise suppressor, with the level of penalisation controlled by the penalisation factor beta, set by the user. The Q.Clear algorithm also includes point spread function (PSF) modelling. Studies have shown that BPL increases the apparent level of FDG uptake particularly in small lesions compared to OSEM [10-12]. This may potentially have a significant impact on the classification of FDG uptake within SPNs according to the BTS guidelines by increasing FDG uptake within a SPN to a greater degree than that of reference soft tissues, e.g. mediastinal blood pool (MBP), with resultant increases in the estimated risk of malignancy generated by the Herder model. The aim of this study is to investigate the effect of BPL, in comparison with OSEM, on the qualitative assessment of FDG uptake and resultant estimation of malignancy risk (Herder score) in SPNs assessed using the Herder model according to the current BTS guidelines.

## **Methods:**

### *Inclusion criteria*

Patients who underwent FDG PET-CT assessment of their SPN between January 2014-December 2017 were identified through institutional databases.

Eligible patients fulfilled the following criteria:

- FDG PET-CT examination performed on a GE 710 PET-CT system (GE Healthcare, Chicago, IL, USA) with assessable OSEM and BPL PET reconstructions.
- SPNs measuring  $\geq 5\text{mm}$  and  $\leq 30\text{mm}$  in size.
- Histological confirmation obtained either via percutaneous biopsy or surgical resection for all malignant nodules.
- Histological confirmation, unchanged morphological appearances on CT follow-up (either by mean diameter for a minimum of 2 years, or by volumetric analysis for a minimum of 1 year) or resolution on follow-up imaging, for all benign nodules.

An institutional board review approval was obtained for this retrospective analysis.

### *FDG PET-CT imaging protocol*

All FDG PET-CT examinations were performed on one of two institutional GE 710 PET-CT systems. Patients were fasted for a minimum of 6 hours. A standard PET acquisition from skull base to upper thighs was acquired post-injection of 350MBq ( $\pm 10\%$ ) of FDG with an axial field view of 15.7cm and an 11 slice overlap at 3 minutes per bed position. The mean tracer uptake time was  $84 \pm 10$  minutes (range 59-99 minutes). Non-attenuation corrected and attenuation corrected datasets were reconstructed. The low-dose unenhanced CT component was performed with patients maintaining normal shallow respiration, using a standardised protocol with the following settings: 140kV, pitch 1.375, 40mm beam collimation in the z-axis corresponding with the detector bank length (64 x 0.625 mm) with an effective slice collimation of 0.625 mm, 0.5s rotation time, Auto mA (15-100mA, noise index 40). CT images were reconstructed with a slice thickness of 2.5mm.

## PET reconstructions

The standard clinical PET reconstruction was a Time of Flight OSEM reconstruction using 2 iterations, 24 subsets and a 6.4mm Gaussian filter (VPFX, GE Healthcare). The archived raw data sinograms were retrospectively reconstructed using the novel BPL algorithm (Q.clear, GE Healthcare) with the established penalisation factor (beta) of 400, which has been identified to be the optimal penalty factor for FDG PET-CT imaging in oncology from previous studies [10-13]. PET images were reconstructed with a slice thickness of 3.27mm and pixel size of 4.7mm.

## FDG PET-CT imaging review

Image analysis was undertaken independently by a PET-CT fellow (DJM) and a consultant radionuclide radiologist (MS) with 2 and 7 years of experience in PET-CT reporting, respectively. Qualitative and semi-quantitative analysis was performed on both PET reconstructions by both readers in a random order, blinded to the clinical information. Qualitative assessment of FDG uptake within SPNs was assigned a score according to the BTS score (**Table 1, Figure 1**). Although not explicitly mandated by Herder et al. [3] or BTS guidelines [1], semi-quantitative measures of FDG uptake, i.e.  $SUV_{max}$ , were used to help confirm the qualitative assessment and classification of FDG uptake in SPNs using the BTS scale. A freehand ROI was outlined in the arch of the aorta, careful to avoid the aortic walls, to define  $SUV_{max}$  MBP, whilst a large freehand ROI was outlined in the right lobe of the liver to define  $SUV_{max}$  hepatic activity, ignoring any voxels that contained spuriously elevated  $SUV_{max}$  values. We chose to measure MBP and hepatic  $SUV_{max}$ , as  $SUV_{max}$  is easily available, has good inter-reader reproducibility, and is relatively unaffected by partial volume averaging [14], and is recommended in the lymphoma literature as standard methodology regarding the Deauville criteria [15]. Scans with disagreement in BTS score between the two readers had consensus reads for both reconstructions. Once FDG uptake in all SPNs was classified, the estimated risk of malignancy was calculated for each SPN using the Herder model [3,16] for both PET reconstructions, as follows:

$$\text{Herder model} = 1/(1 + e^{-x}),$$

where  $x = -4.739 + 3.691$  (% probability by the model of Swensen *et al* [17] ) + 2.322 (BTS score 2) + 4.617 (BTS score 3) + 4.771 (BTS score 4);  $e$  is the base of natural logarithms; the level of nodule FDG uptake (BTS score) is denoted as 1 for present and 0 for absent. The Swenson model is as follows:

$$\text{Swensen model} = 1/(1 + e^{-x}),$$

where  $x = -6.8272 + 0.0391$  (age in years) + 0.7917 (cigarettes) + 1.3388 (cancer history) + 0.1274 (diameter) + 1.0407 (spiculation) + 0.7838 (upper lobe); cigarettes is 1 if current/former smoker, otherwise 0; cancer history is 1 if the patient has a history of extra-thoracic cancer; spiculation is 1 if the nodule is spiculated and upper lobe is 1 if the nodule has an upper lobe location.

### Statistical analysis

Continuous variables are presented as mean  $\pm$  standard deviation (SD). Categorical variables are presented as frequencies and percentages. Group comparison of continuous variables was performed using the Student's t-test. Group comparisons of categorical variables were performed using the Wilcoxon matched-pairs test. A value of  $P < 0.05$  was considered significant. Inter-observer agreement for each PET reconstruction was assessed as follows. Firstly, the agreement between the categorised BTS scores was examined. Due to the ordinal nature of these categories, the weighted kappa method was used to assess agreement as follows: 0.81-1.00= very good agreement; 0.61- 0.80=good agreement, 0.41-0.60 =moderate agreement; 0.21- 0.4= fair agreement [18] . Secondly, the agreement between observers for the continuous Herder scores was examined using the intra-class coefficient (ICC) method. Bootstrapping methods were used to calculate a confidence interval for the difference in the level of agreement between the two PET reconstructions. For each PET reconstruction, the diagnostic performance of the continuous Herder score was determined by calculating the area under the ROC curve (AUC) [19]. The AUCs from the two PET reconstructions were compared using methods of comparing correlated ROC curves [20]. ROC curves were also generated for SPN SUV<sub>max</sub> for each PET reconstruction using the averaged SPN SUV<sub>max</sub> between the two readers. The ROC curve results were analysed to determine the sensitivity, specificity, positive and negative predictive values for a series of pre-defined Herder score cut-off points (0.1, 0.5 and



0.7), and to determine the optimum SPN SUV<sub>max</sub> cut-off value. Confidence intervals were calculated using the exact binomial method.

- 1
- 2
- 3
- 4
- 5
- 6
- 7
- 8
- 9
- 10
- 11
- 12
- 13
- 14
- 15
- 16
- 17
- 18
- 19
- 20
- 21
- 22
- 23
- 24
- 25
- 26
- 27
- 28
- 29
- 30
- 31
- 32
- 33
- 34
- 35
- 36
- 37
- 38
- 39
- 40
- 41
- 42
- 43
- 44
- 45
- 46
- 47
- 48
- 49
- 50
- 51
- 52
- 53
- 54
- 55
- 56
- 57
- 58
- 59
- 60
- 61
- 62
- 63
- 64
- 65

## Results

### *Clinical and nodule characteristics (Table 2)*

Ninety-seven patients (47 female, 50 male, mean age  $69 \pm 10$  years) with 97 SPNs met the inclusion criteria. Of the 97 SPNs, 75 (77%) were malignant, and 22 (23%) benign. Malignant SPNs were predominantly non-small cell lung cancers ( $n=67$ , 89%), with extra-thoracic metastasis ( $n=7$ , 9%) and small cell lung cancer ( $n=1$ , 1%) comprising the remainder. Benign aetiologies included infection, mycobacterial granulomata, granulomatous disease and intrapulmonary lymph nodes. The mean SPN size was  $16 \pm 6$  mm (range 5-29 mm), with 20 SPNs (21%) measuring  $\leq 10$  mm in size. Malignant SPNs were significantly larger than benign SPNs ( $17.8 \pm 5.5$  mm vs.  $11.4 \pm 5.3$  mm,  $p=0.0001$ ), and were more likely to be spiculated (49 vs. 5,  $p=0.0005$ ).

### *BTS nodule uptake score*

There was a significant difference in FDG uptake in SPNs classified using the BTS score, between the two PET reconstruction methods, with significantly higher BTS scores observed with BPL compared to OSEM (**Figure 2**,  $p<0.001$ ). 84% of SPNs showed BTS 3 or 4 uptake on BPL, compared to 75% for OSEM. There was concordance in BTS score between the two PET reconstructions in 74% of SPNs ( $n=72$ ) (**Figure 3**); BTS score 1 = 5 SPNs, BTS score 2 = 10 SPNs, BTS score 3 = 26 SPNs, BTS score 4 = 31 SPNs. BPL increased the BTS score in 25 (26%) SPNs (20 malignant, 5 benign) (**Figure 4**); differences in BTS score were only by a single category with 9 SPNs (7 malignant) increasing from BTS score 2 to 3, and 16 (13 malignant) increasing from BTS score 3 to 4 (**Figure 2**). No SPN was categorised as a higher BTS score using OSEM. There was no disagreement between BPL and OSEM in the categorisation of BTS score 1 uptake. The mean diameter of the 25 SPNs that demonstrated an increase in BTS score with BPL was  $13.8 \pm 3.9$  mm (range 8-24 mm), significantly smaller than the mean diameter of  $17.3 \pm 6.4$  mm (range 5-29 mm) in the remainder of the SPNs that were unchanged ( $p=0.015$ ).

### *Herder score (Table 3).*

Commensurate with the overall increase in the level of SPN FDG uptake associated with BPL, the overall mean Herder score was higher for BPL compared to OSEM ( $73 \pm 29\%$  vs.  $68 \pm 32\%$ ,  $p=0.001$ ). The Herder score for malignant SPNs was higher for BPL than OSEM ( $83 \pm 19\%$  vs.  $78 \pm 25\%$ ,  $p=0.004$ ), but not for benign SPNs ( $42 \pm 35\%$  vs.  $37 \pm 34\%$ ,  $p=0.07$ ). For the 9 SPNs that increased from a BTS score 2 to 3, the mean Herder score increase was  $48 \pm 3\%$ , whilst for the 16 SPNs increasing from a BTS score 3 to 4, the mean Herder score increase was only  $2 \pm 1\%$ . Adenocarcinomas comprised 57% ( $n=43$ ) of malignant SPNs and were the only histological subtype to demonstrate a significantly higher Herder score on BPL compared to OSEM images ( $84 \pm 16\%$  vs.  $76 \pm 27\%$ ,  $p=0.005$ ); these results are summarised in **Table 3**.

#### *Nodule $SUV_{max}$ (Table 3).*

Mean nodule  $SUV_{max}$  was significantly higher on the BPL images compared to OSEM for the overall cohort ( $7 \pm 5.2$  g/ml vs  $4.9 \pm 3.5$  g/ml respectively,  $p=0.001$ ), for malignant nodules ( $8.3 \pm 5.1$  g/ml vs  $5.8 \pm 3.5$  g/ml respectively,  $P=0.0004$ ), but not for benign nodules ( $2.4 \pm 1.9$  g/ml vs  $1.8 \pm 1.3$  g/ml respectively,  $p=0.07$ ). There was no significant difference between the two PET reconstructions for measurement of mean MBP  $SUV_{max}$ , or mean liver  $SUV_{max}$ .

#### *Inter-observer agreement*

The inter-observer agreement using the BTS score was very good for both BPL and OSEM, with weighted kappas of 0.89 (95% CI: 0.74, 1.0) and 0.85 (95% CI: 0.71, 0.99), respectively. There was also very good inter-observer agreement using the continuous Herder score for both BPL and OSEM, with an ICC value of 0.98 (95% CI: 0.97, 0.99) for BPL and 0.93 (95% CI: 0.90, 0.95) for OSEM.

#### *Diagnostic performance*

The diagnostic performance of the continuous Herder score (**Figure 5a**) revealed a good performance for both methods, with an AUC of 0.84 for BPL (95% CI: 0.75, 0.93), and 0.83 for OSEM (95% CI 0.74, 0.92) with no statistically significant difference ( $p=0.39$ ). Using a Herder score cut-off of 10%, as proposed by the BTS guidelines, resulted in similar sensitivity and specificity for both techniques (**Table 4**). A Herder score of 50% was more sensitive for BPL than OSEM, but less specific, and a cut-off of 70% yielded similar results

between the two methods. The diagnostic performance of SPN  $SUV_{max}$  (**Figure 5b**) for predicting malignancy, using each PET reconstruction, revealed a good performance of each method, with an AUC of 0.87 for BPL (95% CI: 0.79, 0.94) and 0.88 for OSEM (95% CI: 0.81, 0.96), with no statistically significant difference between the two PET reconstructions ( $p=0.23$ ). There was no statistically significant difference between the diagnostic performance of the Herder score and nodule  $SUV_{max}$  for either OSEM or BPL ( $p=0.09$  and  $0.35$  respectively). The optimum SPN  $SUV_{max}$  cut-off value for BPL was 2.8g/ml (sensitivity 0.87, specificity 0.68, PPV 0.9, NPV 0.6), and for OSEM 2.9g/ml (sensitivity 0.78, specificity 0.82, PPV 0.94, NPV 0.53).

## Discussion

BPL PET reconstruction increased the BTS score by a single category in comparison with OSEM, in 25 (26%) SPNs (20 malignant, 5 benign). SPNs whose BTS score increased with BPL were significantly smaller than those that remained unchanged (mean SPN diameter 13.8mm vs. 17.3mm respectively). Both Teoh et al. [11] and Howard et al. [21] found the greatest increase in  $SUV_{max}$  was in smaller SPNs, particularly those in the 8-15mm range.

BPL enables effective convergence of the image through an increased number of iterations by application of a penalisation factor to suppress image noise [13], which improves quantification and increases  $SUV_{max}$ , particularly in smaller lesions [22]. However, due to PSF modelling in Q.clear, the likelihood of artefacts increases [22]. This phenomenon, known as a Gibb's artefact, is an artefactual increase in uptake at opposite edges of lesions, which in smaller lesions get closer together and overlap at a critical diameter, resulting in an artificial overestimation of intensity of uptake in the centre of the lesion. Yamaguchi et al. [23] showed that although BPL suppresses such artefacts, overestimation of uptake continues in smaller lesions, to a greater degree than OSEM with PSF modelling, resulting in concern that incorrect diagnoses based on SUVs might increase, particularly with lesions ~10mm.

Although the increase in BTS score with BPL translated into an overall significant increase in the Herder score, this did not result in a change in diagnostic accuracy (0.84) compared to OSEM (0.83). Reviewing the 25 SPNs that increased their BTS score with BPL; 16 increased from BTS score 3 to BTS score 4. This results in only a small change in the weighting factor, associated with level of FDG uptake, in the Herder model equation [3], resulting in an average final increase in the Herder score of only 2%. In practice, this is unlikely to result in management change, as nodules with BTS score 3 are already likely to be considered high risk for malignancy, given that BTS guidance advocates further investigation for any SPN with a Herder score of >10% [1]. The 9 SPNs that increased from BTS score 2 to BTS score 3 with BPL did result in a significant increase in the Herder score of 48%, due to an higher weighting factor in the Herder model equation [3]. A near 50% increase in Herder score has the potential to change management, resulting in

more aggressive and invasive management of SPNs, i.e. excision or non-surgical management (+/- image guided biopsy). The overall increase in Herder scores with BPL across the cohort explains the higher sensitivities compared to OSEM using the Herder score cut-offs of 0.5 and 0.7. The BTS guidelines propose a Herder score cut-off of 10%, above which further investigation or biopsy is recommended [1], and both OSEM and BPL demonstrated similar high sensitivities and low specificities at this cut-off of 0.99 and 0.18 respectively. Reassuringly, there was complete agreement between the two methods in determining BTS score 1. Distinguishing between BTS 2 and BTS 3 score in metabolically active SPNs is the most important PET-related factor determining the final Herder score.

There was very good inter-observer agreement using the BTS scale. Herder et al. classified nodule uptake into faint, mild, moderate and intense, but did not define these cut-offs [3]. Al-Ameri et al. assigned  $SUV_{max}$  cut-offs to help classification; no uptake; faint uptake ( $SUV_{max} \leq 2.5g/ml$ ); moderate uptake ( $SUV_{max} 2.6-10g/ml$ ) intense uptake ( $SUV_{max} > 10g/ml$ ) [4]. Assigning strict  $SUV_{max}$  cut-off values can be problematic, due to the myriad of factors that can affect  $SUV_{max}$  readings other than lesional metabolic activity, including blood glucose levels, radiotracer uptake time, scanner type and PET reconstruction algorithm [7]. Internal reference controls, i.e. MBP and hepatic uptake, can overcome some of these reproducibility issues and have been validated in other malignancies [24]. The 2015 BTS guidelines defined the uptake levels proposed by Herder et al. with reference to background lung and MBP uptake [1]. We incorporated  $SUV_{max}$  rather than  $SUV_{mean}$  in these reference regions to help confirm the qualitative BTS scale classification because although  $SUV_{mean}$  may be less influenced by image noise than  $SUV_{max}$ , its reproducibility is more dependent on standardising the location and size of the region of interest than  $SUV_{max}$ , limiting consistency between readers[24].

In our cohort, we found slightly higher AUCs for the diagnostic performance of SPN  $SUV_{max}$  on both OSEM and BPL compared with the Herder model, although the differences were not significant. This may be explained by the high prevalence of malignancy in our cohort of 77% compared with that of 57.5% in that of Herder et al.[3]. A meta-analysis by Gould et al [25]comprising 1474 pulmonary lesions found that

semiquantitative analysis of FDG uptake provided no additional benefit to the diagnostic accuracy achieved through qualitative visual assessment.

There are several advantages to the use of risk prediction models. Firstly, they enable an estimate of malignancy risk based upon several established clinical and imaging predictors of malignancy rather than sole reliance on a single imaging parameter, i.e. SPN FDG uptake. Secondly, the estimation of risk helps guide management strategies with the lowest risk favouring the least invasive approach, i.e. CT surveillance, and vice versa; such practice is supported by data from cost-effectiveness studies [26,27]. Finally, and perhaps most importantly, it facilitates shared decision making between clinicians and patients by helping interpret SPN malignancy risk in the clinical context of risk of potential complications associated with any proposed invasive procedure, such as image-guided biopsy.

Our study has limitations. It is a single centre, retrospective study, with a large malignant cohort of SPNs. Identification of more benign SPNs, was difficult due to a malignant bias in local FDG PET-CT referral patterns, which reflects real world clinical practice. This malignant bias did not however impact our primary aim to investigate the effect of BPL on BTS scale classification and Herder score in SPNs undergoing FDG PET-CT assessment. Inclusion of small nodules, down to 5mm in size, are at the limits of the spatial resolution of PET for accurate characterisation. Histological validation was not available for all benign SPNs, but this again reflects real world practice, where stability on follow-up imaging obviates the need for histological sampling. We used a freehand ROI to measure SPN FDG uptake for BPL and OSEM images; this could potentially introduce operator error in drawing the ROI around the nodule, but this limitation is mitigated by our use of  $SUV_{max}$ , which has lower operator related variability compared with  $SUV_{mean}$  [28]. There was heterogeneity in the tracer uptake time across the cohort, which also has the potential to affect FDG uptake in SPNs, although this effect is difficult to quantify.

## **Conclusion**

Classification of FDG uptake in a SPN as either below (BTS score 2) or above that of the MBP (BTS score 3) is the most important PET-related factor when using the Herder model and can be undertaken with very

good interobserver agreement for both OSEM and BPL. BPL reconstruction did not affect the overall diagnostic performance of the Herder model in comparison with OSEM, but BPL did change the BTS score in 26% of nodules and significantly increased the Herder score compared to OSEM, particularly in nodules ~13mm. Smaller nodules may show increased FDG uptake with BPL due to a better estimation of true uptake but also possibly due to false overestimation due to Gibb's artefact. If using BPL to quantify FDG uptake in a SPN, we recommend having OSEM reconstruction available for simultaneous review. Studies with a larger cohort and a higher proportion of benign SPNs may help determine the optimum Herder score cut-off value to distinguish between benign and malignant SPNs using BPL reconstructed images.



## References

- [1] M.E.J. Callister, D.R. Baldwin, A.R. Akram, S. Barnard, P. Cane, J. Draffan, et al., British Thoracic Society guidelines for the investigation and management of pulmonary nodules, *Thorax*. 70 Suppl 2 (2015) ii1–ii54. doi:10.1136/thoraxjnl-2015-207168.
- [2] A. McWilliams, M.C. Tammemagi, J.R. Mayo, H. Roberts, G. Liu, K. Soghrati, et al., Probability of cancer in pulmonary nodules detected on first screening CT, *N. Engl. J. Med.* 369 (2013) 910–919. doi:10.1056/NEJMoa1214726.
- [3] G.J. Herder, H. van Tinteren, R.P. Golding, P.J. Kostense, E.F. Comans, E.F. Smit, et al., Clinical prediction model to characterize pulmonary nodules: validation and added value of 18F-fluorodeoxyglucose positron emission tomography, *Chest*. 128 (2005) 2490–2496. doi:10.1378/chest.128.4.2490.
- [4] A. Al-Ameri, P. Malhotra, H. Thygesen, P.K. Plant, S. Vaidyanathan, S. Karthik, et al., Risk of malignancy in pulmonary nodules: A validation study of four prediction models, *Lung Cancer*. 89 (2015) 27–30. doi:10.1016/j.lungcan.2015.03.018.
- [5] J.W. Fletcher, S.M. Kymes, M. Gould, N. Alazraki, R.E. Coleman, V.J. Lowe, et al., A comparison of the diagnostic accuracy of 18F-FDG PET and CT in the characterization of solitary pulmonary nodules, *J. Nucl. Med.* 49 (2008) 179–185. doi:10.2967/jnumed.107.044990.
- [6] L. Evangelista, A. Panunzio, R. Polverosi, F. Pomerri, D. Rubello, Indeterminate lung nodules in cancer patients: pretest probability of malignancy and the role of 18F-FDG PET/CT, *AJR Am J Roentgenol.* 202 (2014) 507–514. doi:10.2214/AJR.13.11728.
- [7] M.C. Adams, T.G. Turkington, J.M. Wilson, T.Z. Wong, A systematic review of the factors affecting accuracy of SUV measurements, *AJR Am J Roentgenol.* 195 (2010) 310–320. doi:10.2214/AJR.10.4923.
- [8] S. Tong, A.M. Alessio, P.E. Kinahan, Image reconstruction for PET/CT scanners: past achievements and future challenges, *Imaging Med.* 2 (2010) 529–545. doi:10.2217/iim.10.49.
- [9] General Electric (GE). GE Healthcare White Paper: Q.Clear .2014. Available from: <https://www.gehealthcare.com/-/media/739d885baa59485aaef5ac0e0eeb44a4.pdf>. Accessed 12/1/2019.
- [10] E.J. Teoh, D.R. McGowan, K.M. Bradley, E. Belcher, E. Black, A. Moore, et al., 18F-FDG PET/CT assessment of histopathologically confirmed mediastinal lymph nodes in non-small cell lung cancer using a penalised likelihood reconstruction, *Eur Radiol.* 26 (2016) 4098–4106. doi:10.1007/s00330-016-4253-2.
- [11] E.J. Teoh, D.R. McGowan, K.M. Bradley, E. Belcher, E. Black, F.V. Gleeson, Novel penalised likelihood reconstruction of PET in the assessment of histologically verified small pulmonary nodules, *Eur Radiol.* 26 (2016) 576–584. doi:10.1007/s00330-015-3832-y.
- [12] N. Parvizi, J.M. Franklin, D.R. McGowan, E.J. Teoh, K.M. Bradley, F.V. Gleeson, Does a novel penalized likelihood reconstruction of 18F-FDG PET-CT improve signal-to-background in colorectal liver metastases? *Eur J Radiol.* 84 (2015) 1873–1878. doi:10.1016/j.ejrad.2015.06.025.
- [13] E.J. Teoh, D.R. McGowan, R.E. Macpherson, K.M. Bradley, F.V. Gleeson, Phantom and Clinical Evaluation of the Bayesian Penalized Likelihood Reconstruction Algorithm Q.Clear on an LYSO PET/CT System, *J. Nucl. Med.* 56 (2015) 1447–1452. doi:10.2967/jnumed.115.159301.
- [14] P.E. Kinahan, J.W. Fletcher, Positron emission tomography-computed tomography standardized uptake values in clinical practice and assessing response to therapy, *Semin. Ultrasound CT MR.* 31 (2010) 496–505. doi:10.1053/j.sult.2010.10.001.
- [15] S.F. Barrington, R. Kluge, FDG PET for therapy monitoring in Hodgkin and non-Hodgkin lymphomas, *Eur. J. Nucl. Med. Mol. Imaging.* 44 (2017) 97–110. doi:10.1007/s00259-017-3690-8.
- [16] British Thoracic Society. BTS Pulmonary Nodule Risk Prediction Calculator 2016. Available from: [www.brit-thoracic.org.uk/standards-of-care/guidelines/bts-guidelines-for-](http://www.brit-thoracic.org.uk/standards-of-care/guidelines/bts-guidelines-for-)

the-investigation-and-management-of-pulmonary-nodules/bts-pulmonary-nodule-risk-prediction-calculator/ Accessed 12/1/2019.

- [17] S.J. Swensen, M.D. Silverstein, D.M. Ilstrup, C.D. Schleck, E.S. Edell, The probability of malignancy in solitary pulmonary nodules. Application to small radiologically indeterminate nodules, *Arch. Intern. Med.* 157 (1997) 849–855.
- [18] J.R. Landis, G.G. Koch, The measurement of observer agreement for categorical data, *Biometrics.* 33 (1977) 159–174.
- [19] J.V. Carter, J. Pan, S.N. Rai, S. Galandiuk, ROC-ing along: Evaluation and interpretation of receiver operating characteristic curves, *Surgery.* 159 (2016) 1638–1645. doi:10.1016/j.surg.2015.12.029.
- [20] E.R. DeLong, D.M. DeLong, D.L. Clarke-Pearson, Comparing the areas under two or more correlated receiver operating characteristic curves: a nonparametric approach, *Biometrics.* 44 (1988) 837–845.
- [21] B.A. Howard, R. Morgan, M.P. Thorpe, T.G. Turkington, J. Oldan, O.G. James, et al., Comparison of Bayesian penalized likelihood reconstruction versus OS-EM for characterization of small pulmonary nodules in oncologic PET/CT, *Annals of Nuclear Medicine.* 31 (2017) 623–628. doi:10.1007/s12149-017-1192-1.
- [22] C.S. van der Vos, D. Koopman, S. Rijnsdorp, A.J. Arends, R. Boellaard, J.A. van Dalen, et al., Quantification, improvement, and harmonization of small lesion detection with state-of-the-art PET, *Eur. J. Nucl. Med. Mol. Imaging.* 44 (2017) 4–16. doi:10.1007/s00259-017-3727-z.
- [23] S. Yamaguchi, K. Wagatsuma, K. Miwa, K. Ishii, K. Inoue, M. Fukushima, Bayesian penalized-likelihood reconstruction algorithm suppresses edge artifacts in PET reconstruction based on point-spread-function, *Phys Med.* 47 (2018) 73–79. doi:10.1016/j.ejmp.2018.02.013.
- [24] S.F. Barrington, N.G. Mikhaeel, L. Kostakoglu, M. Meignan, M. Hutchings, S.P. Müller, et al., Role of imaging in the staging and response assessment of lymphoma: consensus of the International Conference on Malignant Lymphomas Imaging Working Group, in: *J. Clin. Oncol.* 2014; pp. 3048–3058. doi:10.1200/JCO.2013.53.5229.
- [25] M.K. Gould, C.C. Maclean, W.G. Kuschner, C.E. Rydzak, D.K. Owens, Accuracy of positron emission tomography for diagnosis of pulmonary nodules and mass lesions: a meta-analysis, *JAMA.* 285 (2001) 914–924.
- [26] S.S. Gambhir, J.E. Shepherd, B.D. Shah, E. Hart, C.K. Hoh, P.E. Valk, et al., Analytical decision model for the cost-effective management of solitary pulmonary nodules, *J. Clin. Oncol.* 16 (1998) 2113–2125. doi:10.1200/JCO.1998.16.6.2113.
- [27] C. Lejeune, K. Al Zahouri, M.-C. Woronoff-Lemsi, P. Arveux, A. Bernard, C. Binquet, et al., Use of a decision analysis model to assess the medicoeconomic implications of FDG PET imaging in diagnosing a solitary pulmonary nodule, *Eur J Health Econ.* 6 (2005) 203–214. doi:10.1007/s10198-005-0279-0.
- [28] Y.-E. Huang, C.-F. Chen, Y.-J. Huang, S.D. Konda, D.E. Appelbaum, Y. Pu, Interobserver variability among measurements of the maximum and mean standardized uptake values on (18)F-FDG PET/CT and measurements of tumor size on diagnostic CT in patients with pulmonary tumors, *Acta Radiol.* 51 (2010) 782–788. doi:10.3109/02841851.2010.497772.

## Tables

**Table 1. The BTS scale for classification of FDG uptake in SPNs**

**Table 2. Basic patient and nodule characteristics**

**Table 3. Mean Herder scores & nodule SUV<sub>max</sub> for BPL and OSEM reconstructions**

OSEM= Ordered Subset Expected Maximisation; BPL=Bayesian Penalisation Likelihood; NSCLC=non-small cell lung cancer; NOS=not otherwise specified.

**Table 4. Comparison of diagnostic abilities of OSEM and BPL reconstructions using pre-defined Herder score cut-off points**

OSEM= Ordered Subset Expected Maximisation; BPL=Bayesian Penalisation Likelihood; PPV=positive predictive value; NPV=negative predictive value.

## Figure Legend

### Figure 1. Sample OSEM PET images for the BTS score (SUV scale 0-6 g/ml)

1A. BTS score 1=No uptake. Axial image showing uniform uptake in the lung parenchyma, with no increased uptake seen in the 10mm right upper lobe (RUL) nodule (not visible)

1B. BTS score 2=Faint. Axial image showing faint FDG uptake in a 12mm right lower lobe (RLL) nodule (arrow). Nodule  $SUV_{max} = 1.4$  g/ml; Mediastinal blood pool  $SUV_{max} = 1.9$  g/ml.

1C. BTS score 3=Moderate. Axial image showing moderate FDG uptake in a 18mm left lower lobe (LLL) nodule (arrow). Nodule  $SUV_{max} = 2.6$  g/ml; Mediastinal blood pool  $SUV_{max} = 1.8$  g/ml.

1D. BTS score 4=Intense. Coronal image showing intense FDG uptake in a 22mm LLL nodule (arrow). Nodule  $SUV_{max} = 6.9$  g/ml; Liver  $SUV_{max} = 2.9$  g/ml.

### Figure 2. Comparison of SPN FDG uptake levels (BTS score) between OSEM and BPL reconstructions.

BTS=British Thoracic Society; OSEM= Ordered Subset Expected Maximisation; BPL=Bayesian Penalisation Likelihood

### Figure 3. Example of a SPN which showed the same level of uptake on both OSEM and BPL reconstructed PET images

3A. Coronal CT image on lung windows showing a 13mm RUL nodule (arrow).

3B. Coronal OSEM PET image showing faint FDG uptake in the RUL nodule (arrow); BTS score 2. Nodule  $SUV_{max} = 1.5$  g/ml; Mediastinal blood pool  $SUV_{max} = 2.0$  g/ml (SUV scale 0-6 g/ml).

3C. Coronal BPL PET image showing faint FDG uptake in the RUL nodule (arrow); BTS score 2. Nodule  $SUV_{max} = 1.6$  g/ml; Mediastinal blood pool  $SUV_{max} = 1.9$  g/ml (SUV scale 0-6 g/ml).

**Figure 4. Example of a nodule which showed increased uptake on BPL compared to OSEM PET reconstructed images**

4A. Axial CT image on lung windows showing an 8mm LUL nodule (arrow).

4B. Axial OSEM PET image showing faint uptake in the LUL nodule (arrow); BTS score 2. Nodule  $SUV_{max}=0.9$  g/ml, mediastinal blood pool  $SUV_{max}=1.2$  g/ml (SUV scale 0-6 g/ml).

4C. Axial BPL PET image showing moderate uptake in the LUL nodule (arrow); BTS score 3. Nodule  $SUV_{max}=1.9$  g/ml, mediastinal blood pool  $SUV_{max}=1.1$  g/ml (SUV scale 0-6 g/ml).

## **Figure 5**

**Figure 5a ROC curves for the diagnostic performance of the Herder score for predicting malignancy in SPNs, using both BPL and OSEM PET reconstructions.**

OSEM= Ordered Subset Expected Maximisation; BPL=Bayesian Penalisation Likelihood

**Figure 5b. ROC curves for the diagnostic performance of SPN  $SUV_{max}$  for predicting malignancy using both BPL and OSEM PET reconstructions.**

OSEM= Ordered Subset Expected Maximisation; BPL=Bayesian Penalisation Likelihood

***Acknowledgments***

**Role of Funding Source:** The authors acknowledge support from the King’s College London / University College London Comprehensive Cancer Imaging Centres funded by Cancer Research UK and Engineering and Physical Sciences Research Council in association with the Medical Research Council and the Department of Health (C1519/A16463) and the Wellcome Trust EPSRC Centre for Medical Engineering at King’s College London (WT203148/Z/16/Z).

Table 1. The BTS ordinal scale for classification of FDG uptake in SPNs

SPN uptake	BTS score	Definition of FDG uptake in SPN	Definition of SPN SUV <sub>max</sub>
Absent	1	≤ background lung tissue	= background lung tissue SUV <sub>max</sub>
Faint	2	≤ MBP	> background lung tissue SUV <sub>max</sub> but ≤ MBP SUV <sub>max</sub>
Moderate	3	> MBP	> MBP SUV <sub>max</sub> but ≤ 2 times hepatic SUV <sub>max</sub>
Intense	4	Markedly > MBP	> 2 times hepatic SUV <sub>max</sub>

BTS= British Thoracic Society; FDG= 2-deoxy-2-[<sup>18</sup>F]fluoro-D-glucose; SPN= solitary pulmonary nodule; MBP= mediastinal blood pool; SUV<sub>max</sub> = maximum standardised uptake value.

Table 2. Basic patient and nodule characteristics

Patient demographics (n=97)	Overall n ± SD (%)	Benign (n=22, 23%)	Malignant (n=75, 77%)	P value
Mean Age (years)	69 ± 10	70.9 ± 9.4	67.1 ± 14.8	0.25
Female	47 (48%)	9 (41%)	38 (51%)	0.47
Current/former smoker	81 (84%)	16 (73%)	65 (87%)	0.19
Previous malignancy	27 (28%)	5 (23%)	22 (29%)	0.6
Nodule characteristics				
Mean nodule diameter (mm)	16 ± 6	11.4 ± 5.3	17.8 ± 5.5	0.0001
Upper lobe	51 (53%)	12 (55%)	39 (52%)	1
Spiculated	54 (56%)	5 (23%)	49 (65%)	0.0005



**Table 3. Mean Herder scores & nodule SUV<sub>max</sub> for BPL and OSEM reconstructions**

<b>Mean Herder scores (% risk malignancy)</b>			
<b>Grouping (n)</b>	<b>OSEM (% ± SD)</b>	<b>BPL (% ± SD)</b>	<b>P value</b>
Overall (97)	68 ± 32	73 ± 29	0.0011
Malignant (75)	78 ± 25	83 ± 19	0.0039
Benign (22)	37 ± 34	42 ± 35	0.07
<b>Malignant nodules (n, %)</b>			
Adenocarcinoma (43, 57%)	76 ± 27	84 ± 16	0.005
Squamous (15, 20%)	91 ± 6	92 ± 6	0.3
Carcinoid (5, 7%)	66 ± 13	68 ± 13	0.2
NSCLC, NOS (4, 5%)	82 ± 10	82 ± 10	1
Small cell (1, 1%)	80	80	1
Metastasis (7, 9%)	67 ± 38	67 ± 39	0.3
<b>Mean Nodule SUV<sub>max</sub></b>	<b>OSEM (g/ml ± SD)</b>	<b>BPL (g/ml ± SD)</b>	<b>P value</b>
Overall (95)	4.9 ± 3.5	7 ± 5.2	0.001
Malignant (75)	5.8 ± 3.5	8.3 ± 5.1	0.0004
Benign (22)	1.8 ± 1.3	2.4 ± 1.9	0.2

OSEM= Ordered Subset Expected Maximisation; BPL=Bayesian Penalisation Likelihood;

NSCLC=non-small cell lung cancer; NOS=not otherwise specified.

**Table 4. Comparison of diagnostic abilities of OSEM and BPL reconstructions using pre-defined Herder score cut-off points**

<b>Herder score (%)</b>	<b>Statistic</b>	<b>OSEM Estimate (95% CI)</b>	<b>BPL Estimate (95% CI)</b>
10	Sensitivity	0.99 (0.93, 1.00)	0.99 (0.93, 1.00)
	Specificity	0.18 (0.05, 0.40)	0.18 (0.05, 0.40)
	PPV	0.80 (0.71, 0.88)	0.80 (0.71, 0.88)
	NPV	0.80 (0.28, 1.00)	0.80 (0.28, 1.00)
50	Sensitivity	0.87 (0.77, 0.93)	0.96 (0.89, 0.99)
	Specificity	0.64 (0.41, 0.83)	0.55 (0.32, 0.76)
	PPV	0.89 (0.80, 0.95)	0.88 (0.79, 0.94)
	NPV	0.58 (0.37, 0.78)	0.80 (0.52, 0.96)
70	Sensitivity	0.77 (0.66, 0.86)	0.83 (0.72, 0.90)
	Specificity	0.68 (0.45, 0.86)	0.68 (0.45, 0.86)
	Positive PV	0.89 (0.79, 0.96)	0.90 (0.80, 0.96)
	NPV	0.47 (0.29, 0.65)	0.54 (0.34, 0.73)

OSEM= Ordered Subset Expected Maximisation; BPL=Bayesian Penalisation Likelihood;

PPV=positive predictive value; NPV=negative predictive value.

**Figure 1**  
[Click here to download high resolution image](#)

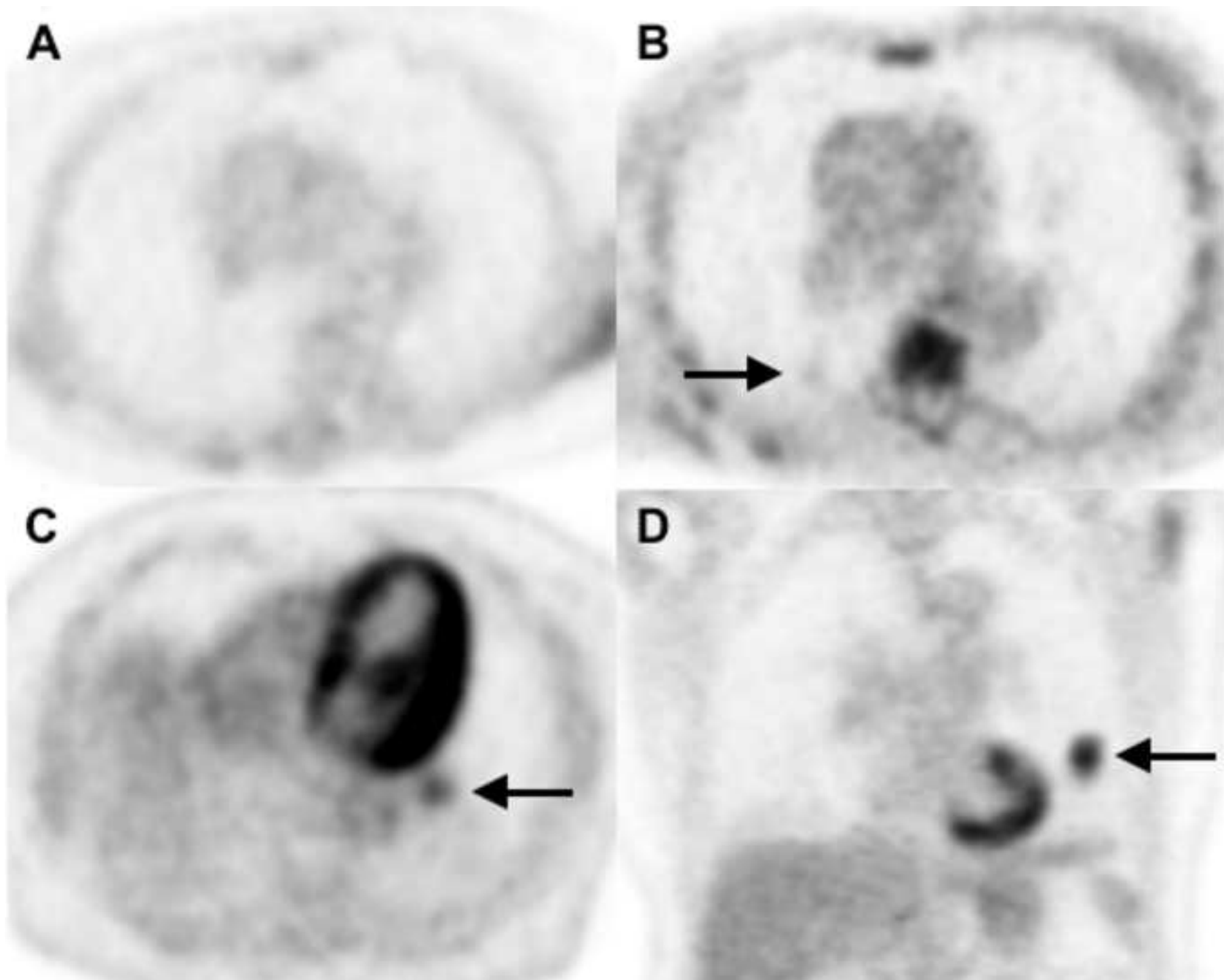
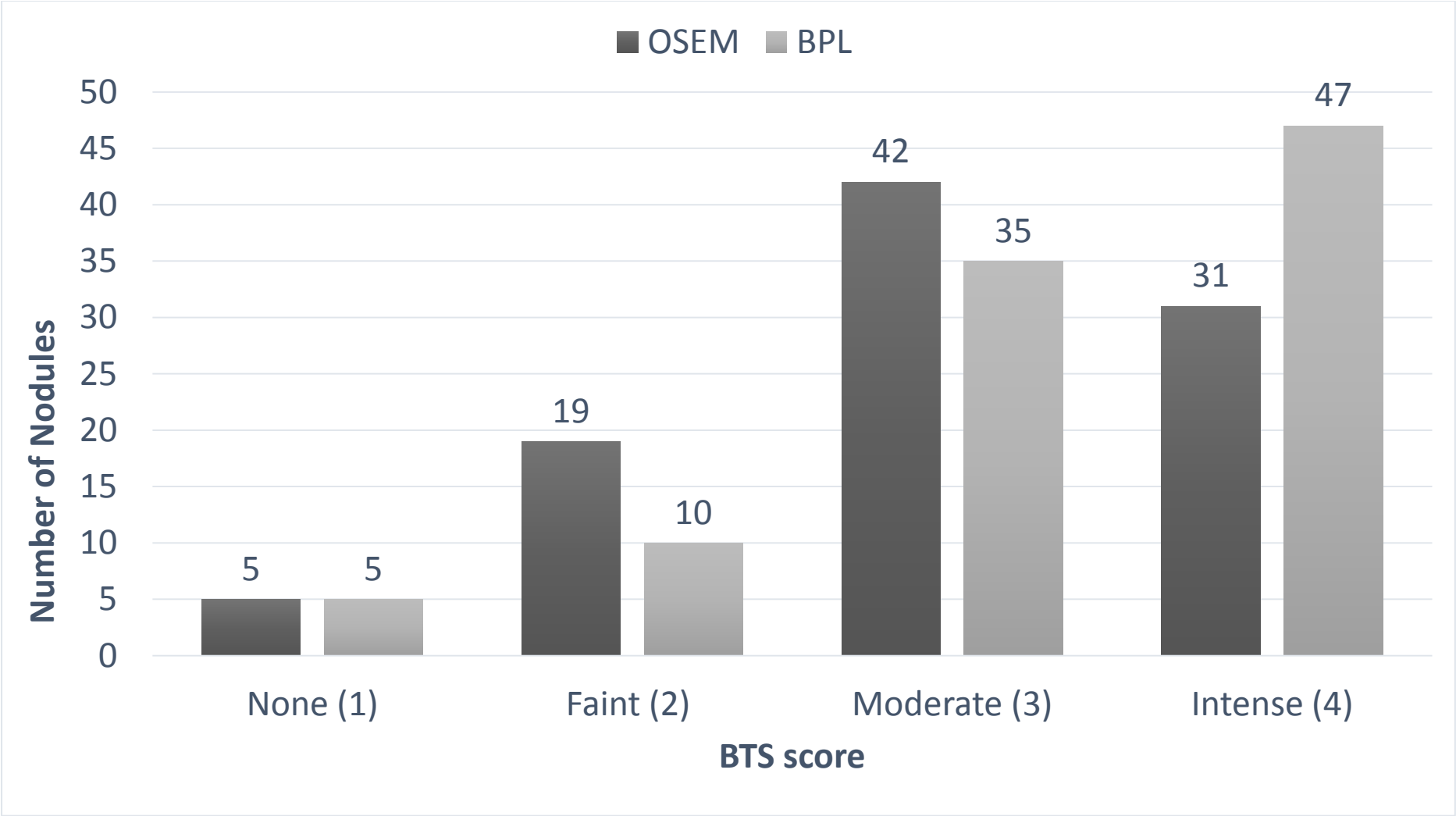
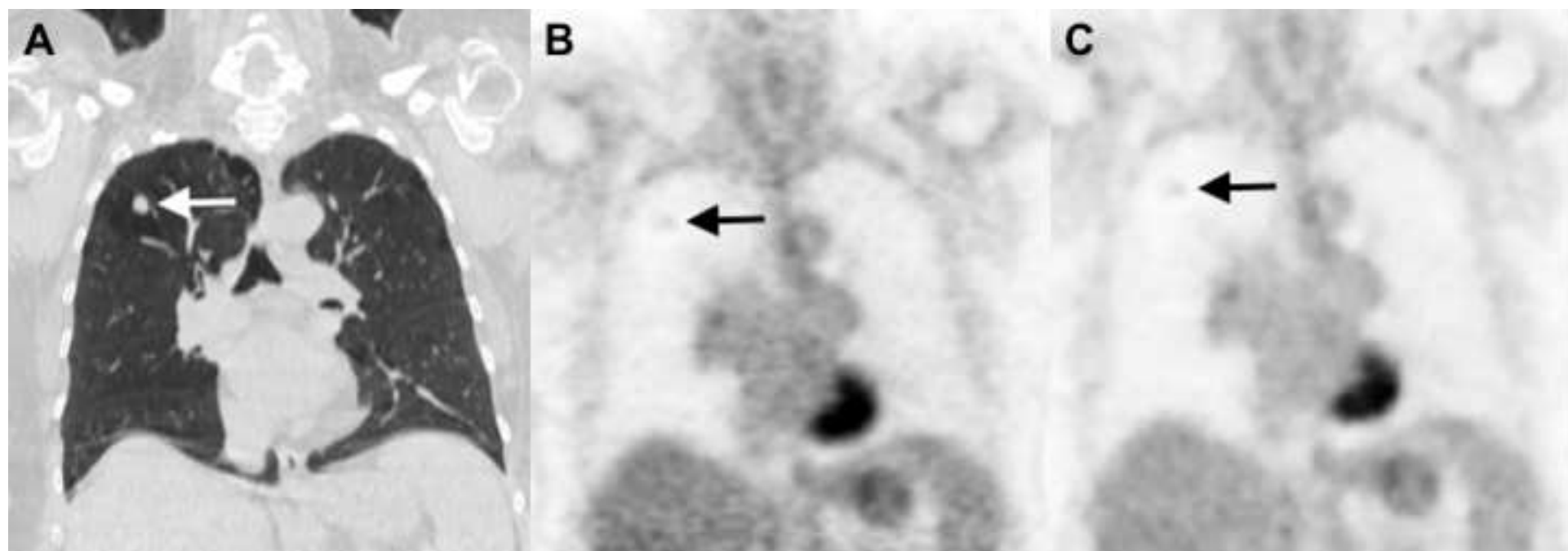


Figure 2



**Figure 3**  
[Click here to download high resolution image](#)



**Figure 4**  
[Click here to download high resolution image](#)

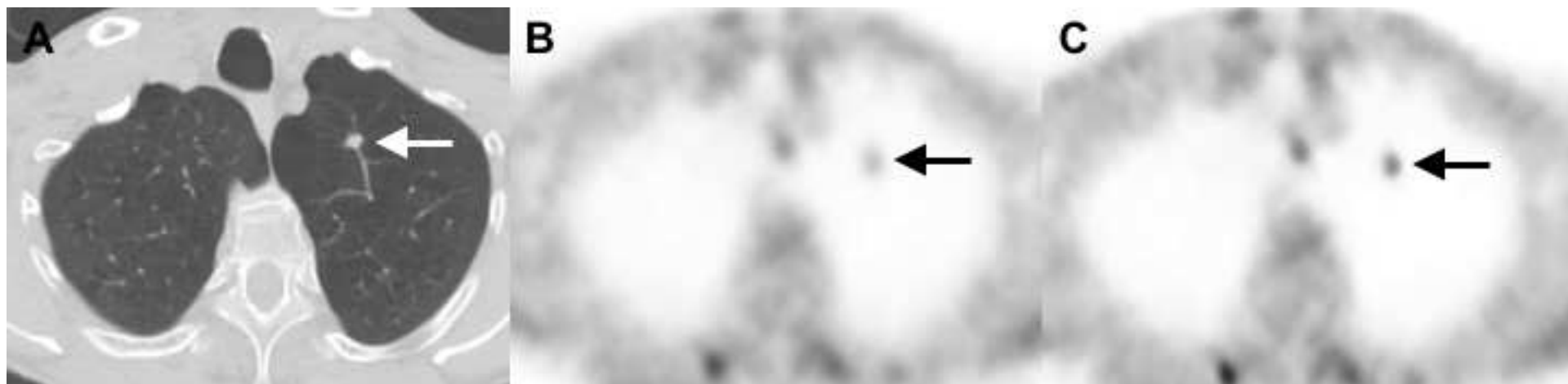


Figure 5a

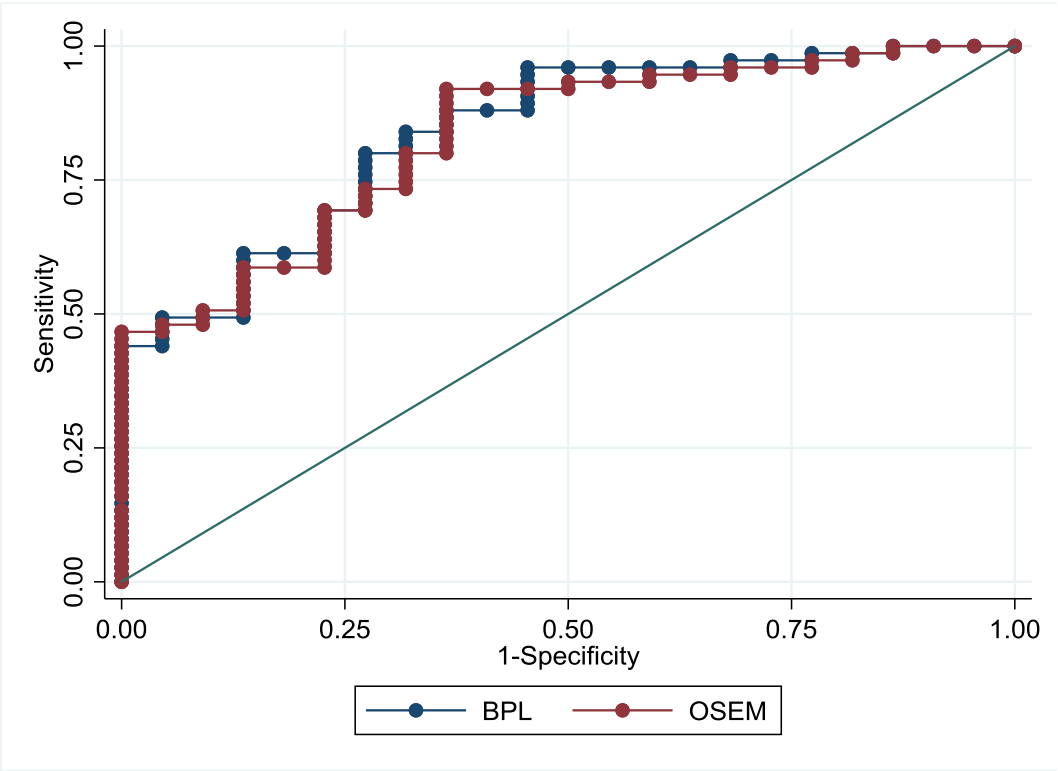
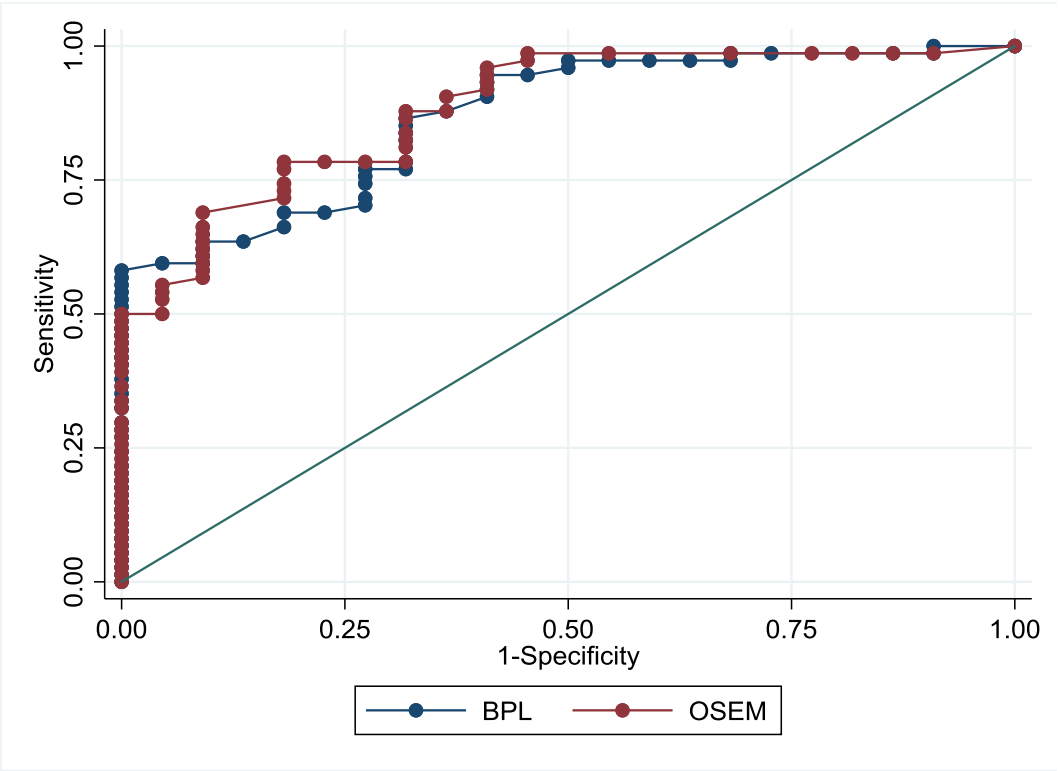


Figure 5b





**Manuscript track changes**

[Click here to download Supplementary File\(s\): BPL SPN EJR\\_resub\\_track\\_5\\_15\\_19.docx](#)